Geometric accuracy evaluation of the new VERO stereotactic body radiation therapy system

Tom Depuydt, Olivier C. L. Haas, Dirk Verellen, Stephan Erbel, Mark De Ridder, Guy Storme

Original citation:
Tom Depuydt, Olivier C. L. Haas, Dirk Verellen, Stephan Erbel, Mark De Ridder, Guy Storme (2010) Geometric accuracy evaluation of the new VERO stereotactic body radiation therapy system. *UKACC International Conference on CONTROL* IET, 259-264. DOI: 10.1049/ic.2010.0291

ISBN: 978-1-84600-038-6

http://dx.doi.org/10.1049/ic.2010.0291

Geometric accuracy evaluation of the new VERO stereotactic body radiation therapy system

Tom Depuydt*, Olivier C. L. Haas, Dirk Verellen*, Stephan Erbel***, Mark De Ridder*, Guy Storme***

** Radiotherapy department, University Hospital UZ Brussel, Belgium (Tel: +32 2 474 90 89, email: tom.depuydt@uzbrussel.be)*
***Control Theory and Applications Centre, Coventry University, UK (Tel: +44 24 7688 7658, o.haas@coventry.ac.uk)*
**** BrainLAB AG, FeldKirchen,,DE*

Abstract: Real-time tracking of moving tumors is one of today's challenges in radiation therapy. This work investigates the tracking performance of VERO, a novel treatment device with gimbaled linear accelerator, especially designed for four dimensional image guided radiotherapy. It is found that the significant impact of organ motion on dose distribution can be overcome by combining a polynomial predictor with a prediction horizon of 50ms with the VERO tracking system. Tracking errors can be reduced from 1.7mm to 0.6mm for realistic patient signals as well as sine wave from 5 to 30 bpm.

Keywords: radiotherapy, tracking, measurements, position accuracy, medical robot

1. INTRODUCTION

In radiation therapy, intra-fraction motion results in significant geometric and dosimetric uncertainties in the therapeutic dose delivery treating thoracic and abdominal tumors. To accommodate these issues and to assure adequate dosimetric coverage of the tumor, geometric safety margins can be introduced which incorporate the entire motion. However, the use of large margins, where healthy tissues are present, prevents dose escalation as the dose to the healthy tissue would be a limiting factor. Tumour dose escalation has been shown to be beneficial in terms of outcome (Wulf *et al*, 2005; McGarry *et al*, 2005; Komaki et al, 2005) when it can be combined with a decrease in excessive irradiation of surrounding normal tissue and critical structures to minimize complications (Kwa *et al*, 1998, Hernando *et al*, 2001). Beam modulation devices can help deliver complex radiation fields that can accurately conform to the PTV whilst at the same time sparing critical structures. The drawback of such treatments known as IMRT and to a lesser extent conformal radiotherapy is the presence of dose distribution with large gradient between the organs at risk and the tumor. If the tumor moves it could receive a significantly lower dose than planned and the organ at risk a significantly higher dose. Such event could negate the expected benefit of dose shaping and modulation. This paper focuses on one method to address organ motion referred to as real time tumor tracking (RTTT). RTTT is believed to be able to bring together the goals of dose escalation and surrounding tissue sparing for moving tumors.

Most of the current RTTT solutions presented exploit existing radiation therapy equipment in new ways to adapt the tumor motion to the therapeutic beam or adapt the beam to the tumor motion. A first approach is respiratory gating (Verellen *et al*, 2006) where the therapeutic beam is switched on only when the moving tumor is adequately covered and switched off otherwise. A drawback here is that the duty cycle usually is no more than 20 to 30 % which leads to very long treatment times. In an attempt to increase the duty cycle approaches like active breathing control (ABC) Wong *et al*, 1999) or breath-holding techniques Mah *et al*, 2000) have been used. However, patients affected by tumors in lungs and abdomen, where intra-fraction motion is most significant, may experience difficulties even with normal breathing, hence both breath-holding and ABC have limited applicability and may cause discomfort to the patients.

The most technically challenging method with potentially the best result is to accommodate tumor motion during irradiation with a real-time tumor tracking radiation delivery system. The principle is that the tumor should stay in the same relative position with respect to the beam. This can be accomplished by continuous adaptation of the patient/tumor position using the patient support system (PSS) with respect to a static beam or by real-time adaptation of the treatment beam itself to the tumor position. The technical feasibility of using a PSS to compensate for measurable tumour motion with respect to the treatment beam has been demonstrated (DeSouza *et al* , 2006, Skworcow *et al*, 2007, Wilbert J. *et al,* 2008). Whilst some studies seems to indicate that moving patient does not lead to any discomfort and can even be relaxing (Wilbert, 2008), the influence of counteracting part or all the motion on patient/tumor position behavior during this continuous repositioning requires further investigation. Indeed compensation of the motion in one direction may lead to a motion in another direction. Other approaches with a fixed patient position were presented where the dynamic behavior of the PSS were taken over by dynamic operation of the multi-leaf collimator (DMLC) (Keall *et al*, 2006, Sawant

et al, 2008, Tacke *et al*, 2010) or a robotic-arm based linear accelerator gantry (Hoogemann et al, 2009). An important issue in DMLC tracking is the orientation of the tumor motion with respect to the leaf motion direction and the limited speed of the leafs. This introduces a difference in tracking performance between tracking a tumor moving inline or perpendicular to the leaf trajectories. The resulting combination of DMLC intensity modulation and arc therapy could potentially lead to unrealistic specifications for the MLC in terms of dynamics. A decoupling of the tracking motion and the DMLC based intensity modulation, such as that proposed in (Kamino et al, 2006), would therefore seem to be a more promising option. Such an approach has been adopted in the development and installation at UZ Brussel of the VERO system, a novel radiation therapy accelerator platform developed for image guided stereotactic body radiotherapy (SBRT). Key to the success of such system is its ability to actually track organ motion consistently with the required accuracy. The aim of this paper is to assess the tracking capabilities of the VERO system in terms of tracking errors, system tracking lag and the equivalence of pan and tilt gimbals motion. Section 2 of the paper describes the new device and the set up and material adopted to carry out the evaluation of the tracking performance of the machine. Section 3 presents the result with appropriate discussion and Section 4 provides a conclusion.

2. MATERIALS AND METHODS

VERO is a joint product of BrainLAB (BrainLAB AG, Feldkirchen, Germany) and MHI (Mitsubishi Heavy Industries, Tokyo, Japan) (Kamino et al, 2006). The VERO system is a small and light 6 MV C-band linac with an MLC mounted on an O-ring gantry. Two orthogonal gimbals hold the linac-MLC assembly, which allows pan and tilt motions of the linac and the therapeutic beam. This mechanism offers the possibility to perform real-time tracking of moving tumors, decoupled from the DMLC intensity modulation of the dose. The maximum excursion amplitude of the beam axis at the isocenter is 4.4 cm in the isocenter plane (or 2.5°) in both pan and tilt direction. Beside an EPID for MV portal imaging, the VERO system is equipped with two orthogonal kV Imaging systems attached to the O-ring at 45° from the MV beam axis. This imaging system allows simultaneous acquisition of orthogonal X-rays images and fluoroscopy. An ExacTrac (BrainLAB AG, Feldkirchen, Germany) automated infra-red (IR) marker based patient-positioning device is integrated into the VERO system.

2.1 Experimental set up with the Quasar phantom

A prototype of the real-time tumor tracking is currently installed on the system at UZB. This enables the VERO system to actively track an IR marker using the pan and tilt motion of the gimbals system. The VERO tracking prototype setup uses the Polaris camera of the BrainLAB ExacTrac system to track one IR marker in space. The gantry and O-ring angles are 0° at all times and for this experiment the IR marker moves only in a horizontal plane at a source to axis distance (SAD) of 1000 mm. The MLC field size is set to 30 by 30 mm and the light field of the system is switched on - see Fig. 1. This light field projects a square onto a sheet of paper perpendicular to the initial linac axis. Besides showing the beam position, the light field produces a shadow of the followed IR marker on the sheet of paper. The projection of light field and marker shadow are captured from below using a photo camera with movie function (Fig 1). This backlit video of the IR marker provides good contrast between the IR projection and the light field emitted by the machine in place of x-rays. The movie frames are acquired at a frame rate of 30 fps and image size of 960x540 pixels. The MPEG movie frames are converted to bitmap files for further processing.

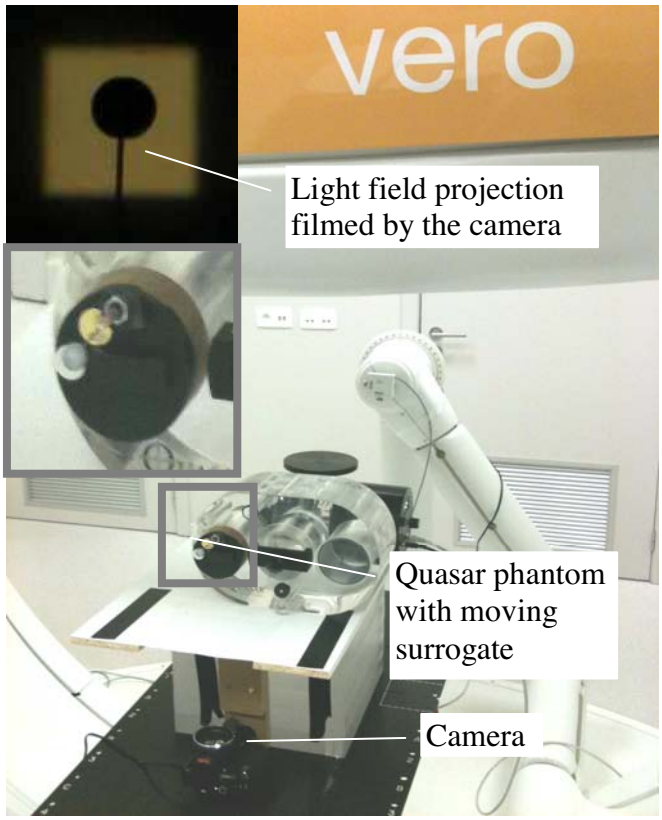

Fig. 1: Experimental setup on the VERO system of the Quasar phantom used to move an IR marker. A camera films the light field projection of the marker to identify the performance of the beam tracking.

2.2 Hough transform for marker and light field tracking

The frames of the movie are analyzed using a Hough transform based feature detection. The IR marker is detected as a circular object in the image, the field outline as a rectangular object. The centroid of the circle is taken as the position of the tracked IR marker object. The centroid of the detected rectangle determines the tracking beam position. For the detection of the tracked object and the tracking beam in the images, a Hough transform (Duda and Heart, 1972) based feature detection algorithm was developed, see Fig. 2. The algorithm includes an edge detector which detects the boundary of the regions of interest by considering the grey levels and applying a threshold. It is followed by a Hough transforms for a circle and a rectangle. The IR marker shadow and the rectangular light field is given by the maximum intensity within the Hough transform images . To

allow sub-pixel accuracy an average value was calculated over the 5 highest values in the Hough transform. To verify the Hough transform feature detection accuracy, video images of the tracked IR marker and the tracking beam were acquired with the tracking mode and Quasar phantom motion switched off. A total of 100 image frames were analyzed with the feature detection algorithm. The standard deviations of the detected circle and rectangle positions were respectively 0.06 mm and 0.04 mm in the static case which was considered adequate.

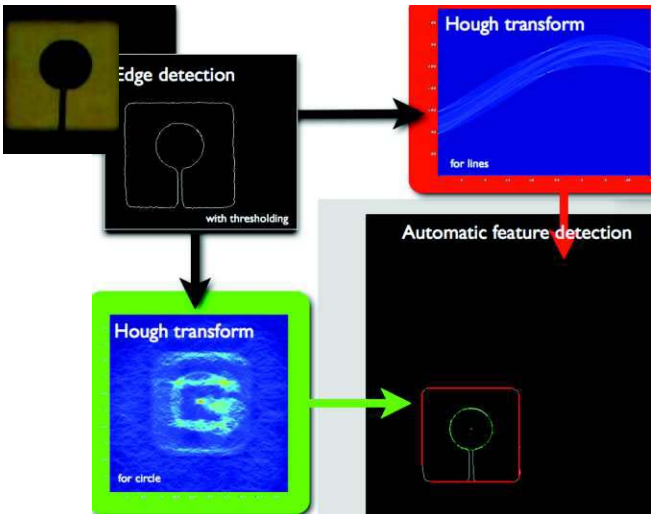

Fig. 2. Illustration of the Hough Transform applied to the backlit moving target and light field

2.3 Tracking motion implementation

To determine the tracking error, an IR marker was placed on the moving part of the Quasar phantom (Modus Medical Devices, London, Canada). A trajectory from a patient as well as a set of one-dimensional sinusoidal motion were produced by the phantom with different frequencies ranging from 5 breaths-per-minute (bpm) (0.085Hz) to 30 bpm (0.5Hz), and a fixed amplitude of 20 mm. The 30 bpm in combination with the 20 mm amplitude reaches the maximal tracking speed of 60 mm/s. The VERO tracking system makes use of a polynomial predictor to anticipate the position of the target being tracked. In this work, a 3rd order polynomial prediction function was selected with a prediction horizon set to 20 ms, 35 ms and 50 ms for all frequencies. To quantify the system lag and be used as a reference a measurement was performed without any form of prediction (i.e. prediction time set to 0 ms). The experiment was performed separately for the X direction or pan and for the Y direction or tilt. The motion of tracked object and tracking beam were recorded simultaneously with the camera system and analyzed with the feature detection algorithm.

2.4 Tracking error and dose blurring

To investigate the relationship between tracking error and dose blurring larger tracking errors were introduced by temporarily reducing the maximum tracking speed from 60 mm/s to 25 mm/s. In a first step the tracking errors were determined in a way identical to what is described in the previous section, using sinusoidal motions of the Quasar phantom. Subsequently the experiment was repeated with the 6 MV beam in tracking mode irradiating an EBT2 radiochromic film inserted in the moving part of the Quasar phantom. Tracking errors result in blurring of the dose distribution. As such a relationship can be established between tracking error and dose blurring due to residual motion of the tracking beam relative to the tumor. Dose blurring was quantified in terms of the penumbra width.

3. RESULTS

The prototype system lag was calculated from the phase shift between the motion of the tracking beam and the motion of the tracked object for a prediction time set to 0 ms. An average was calculated over all applied sinus frequencies from 5 bpm to 30 bpm. A system lag was determined to be 47.7 ms (SD 2.3 ms) and 47.6 ms (SD 2.0 ms) for the X and Y direction respectively. For a forward prediction time of 50 ms, the remaining system lag was -0.2 ms (SD 7.1 ms).

The tracking error was characterized in terms of systematic error, root mean square error (RMSE) and 90% percentile of the absolute tracking error values (E90%) each calculated over a whole number of sinus periods. The maximal systematic errors, calculated as the average of the difference between tracked object and tracking beam position, were below 0.2 mm for all motion sequences. The RMSE and E90% values are shown in Fig. 3 and Fig. 4 for the range of frequencies and for the different forward prediction times.

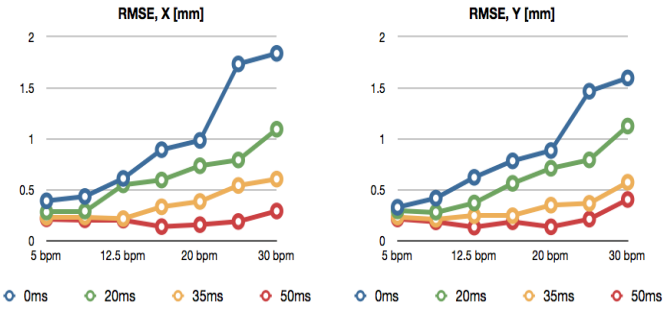

Fig. 3: The root-mean-square tracking error for a range of sinus motions with frequencies from 5 bpm to 30 bpm, for different forward prediction times 0 ms, 20 ms, 35 ms and 50 ms, in X and Y direction

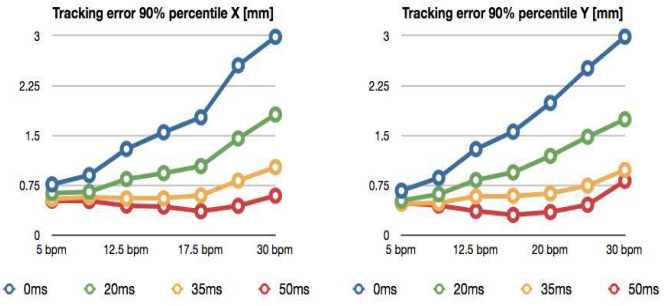

Fig. 4: The 90% percentile (E90%) of the absolute tracking error for a range of sinus motions with frequencies from 5

bpm to 30 bpm, for different forward prediction times 0 ms, 20 ms, 35 ms and 50 ms, in X and Y direction

Without forward prediction, the tracking error is strongly dependent on the motion frequency and values of up to 1.84 mm and 2.98 mm for X and 1.60 mm and 2.99 mm for Y were seen for RMSE and E90% respectively. Compensating the system lag with a forward prediction gimbals control of 50 ms reduced both maximum values of RMSE and E90% respectively to 0.29 mm and 0.59 mm for X, and 0.41 mm and 0.82 mm for Y.

Fig. 5 and 6 illustrate the dynamic behaviour of the beam as well as the reference surrogate marker for the Y axis of motion. In this case a signal obtained from a patient, with an average breathing frequency of 19.1 bpm, was used to provide a realistic range of motion and acceleration. Fig. 5 illustrates the tracking achievable without prediction. Fig. 6 illustrates the improvement that can be achieved with a forward prediction of 50 ms. The RMSE and E90% were respectively 0.95 mm and 1.37 mm without forward prediction, and 0.20 mm and 0.37 mm for 50 ms forward prediction. The tracking behaviour in the X direction for this motion sequence was similar.

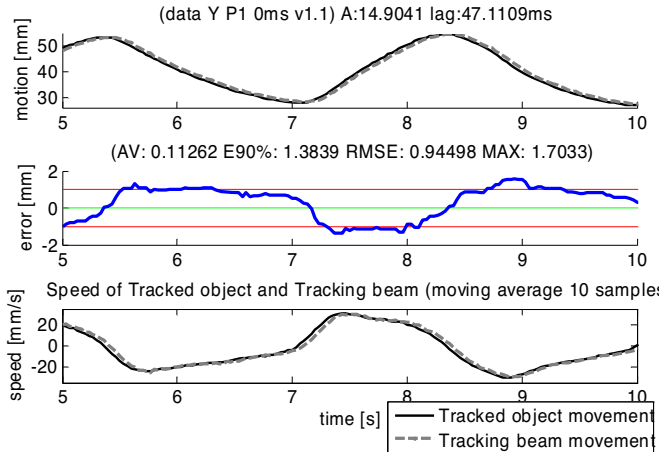

Fig. 5: The movement, tracking error and speed for a patient signal without forward prediction

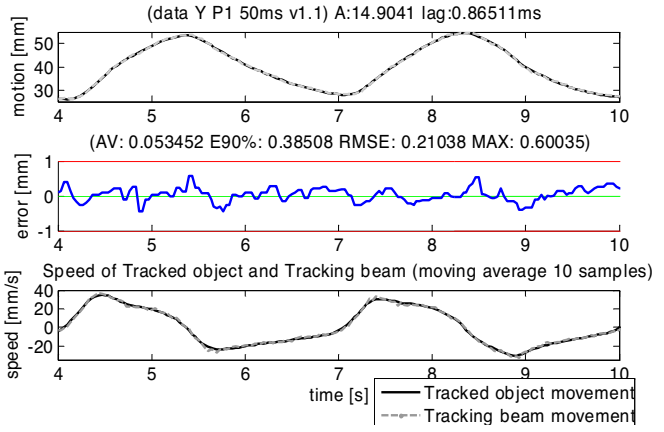

Fig. 6: The movement, tracking error and speed for a patient signal with 50 ms forward prediction

To evaluate the dosimetric effect of the tracking errors an irradiation was carried out where one film was taken without any target motion one without any correction and one using tracking with 50ms prediction illustrated in the left, right and centre film represented in Fig. 7 respectively.

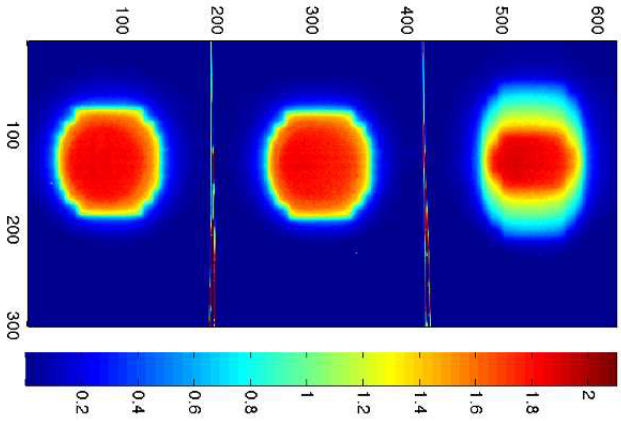

a) Immobile b) Tracked c) Not tracked

Fig. 7: Illustrating the improvement achievable using tracking

Fig. 8 illustrates the influence of the speed of the surrogate marker on the tracking performance in terms of the width of the penumbra region in mm (dose between 20 and 80%) and the high dose region in cm (dose above 80%), determined on a line scan inline with the phantom motion direction. To introduce large tracking errors in this experiment the maximum tracking speed of the prototype was temporarily reduced from 60 mm/s to 25 mm/s. The effect on the irradiation becomes noticeable above 15 bpm when the tracking error is in the order of 1mm RMSE and 1.5mm E90%, because the maximal tracking speed of 25 mm/s is reached.

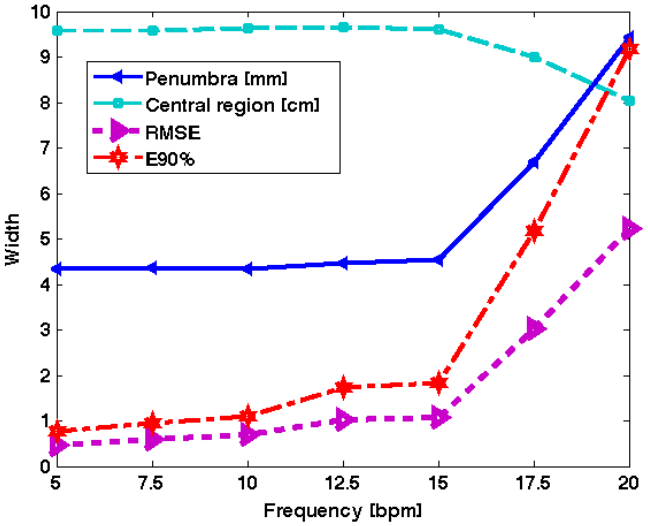

Fig. 8: Illustrating the effect of the number of breath per minute and the speed of the target being tracked on the tracking error in terms of blurring of the dose resulting in increased penumbra (in mm) and reduced high dose region (in cm).

4. DISCUSSION AND CONCLUSIONS

A prototype of a gimbals based tracking system has been tested on a VERO linear accelerator system. It is able to

pursue one IR marker in space with the therapeutic beam. To characterize the tracking performance of the system a series of experiments were conducted to quantify the system latency, tracking error and the equivalence of X and Y motions. The combination of the total system lag of the ExacTrac IR tracking and the gimbals response was experimentally determined to be 47.7 ms. This was in agreement with the sum of the loop sub-system latencies determined independently by the vendor: IR marker position acquisition of 25 ms, gimbals position calculation 2 ms, gimbals control cycle time of 20 ms. For a comparable DMLC tracking setup, using the Varian RPM IR system and Millenium MLC 120 (Varian MS, Palo Alto, CA, US), Keall et al. (2006) have reported a considerably larger total system lag of 160 ms. The IR marker acquisition times were comparable to the ones for ExacTrac, 33 ms versus 25 ms. The MLC control cycle time is 50 ms compared to 20 ms for the VERO gimbals. The leaf position calculation also requires more CPU time than calculation of the gimbals position update. Tacke et al.(2010) have described another DMLC solution based on a Siemens 160 MLC (Siemens AG, Erlangen, Germany) which showed to have a system lag of over 400 ms. The total system latency reported for the CyberKnife (Accuray Inc., Sunnyvale, CA, US) robotic-arm based linear accelerator gantry was 192.5 ms (Hoogeman et al, 2009).

For quantification of the system lag, all the above mentioned tracking loops use an IR based tumor position monitoring with low latencies. These devices and prototypes are not tracking the tumor motion directly based on internal anatomical information or implanted fiducial markers. Clinical tracking systems will most probably use X-ray fluoroscopy for direct tumor tracking, however, not as a sole method because of the extensive imaging dose exposure. The report of AAPM Task Group 76 (Keall et al. 2006) provides an estimate of fluoroscopy exposure to track fiducial gold markers. A dose of 0.18 mGy per image was determined to allow robust detection of the fiducials. If, for example, a stereotactic lung treatment is considered of 15 Gy per fraction, delivering 1500 MU in total with a dose rate of 500 MU/min, this requires 180 s of beam on. A frame rate of 5 times a stereo image per second would result in a considerable imaging exposure of about 0.3 Gy per fraction, primarily of healthy tissues. To overcome this issue, hybrid tumor tracking systems have been proposed, see for example (Hoogeman, 2009), which combine limited X-ray fluoroscopy tracking of internal markers/anatomy with tracking of breathing motion through external markers. Before the treatment delivery is initiated, simultaneous acquisition with both techniques is performed during a calibration sequence and a correlation model between external marker and internal marker motion is determined. The approach during treatment is to use the external markers to feed the actual tumor tracking, but verify at regular time points during treatment the validity of the correlation model with the acquisition of fluoroscopic images. A recalibration of the correlation model can be done during treatment if needed. In that respect, the system latency determined for the currently installed prototype tracking based on external IR markers can be considered relevant for the future clinical released versions of the VERO tracking module when using this hybrid approach.

Real-time tumor tracking using fluoroscopy directly requires a trade-off between different parameters. The additional imaging dose for the patient is determined by the acquisition repetition rate and by the image quality required to allow fast and robust detection of anatomy or implanted fiducials in the images. Low fluoroscopy frame rates will decrease tumor motion temporal information. Additionally, X-ray image acquisition and analysis calculation times will introduce additional system latency in the feedback loop of about 100 ms. Consequently more advanced algorithms for forward prediction will be required which perform well for longer prediction horizons. Further research is required to optimize the balance between adequate temporal information, robust detection and imaging dose for treatment of moving tumors with fluoroscopy based tracking.

The tracking error has been quantified for a set of sinusoidal signals with different frequencies. The error was expressed in both RMSE and E90%. For both metrics increased tracking error was seen in case of inadequate forward prediction. The most appropriate prediction horizon was experimentally found to be 50ms in order to compensate the overall system's latency. The current prototype was able to track the IR marker sinusoidal motion accurately up to frequencies of 30 bpm (0.5 Hz) with an E90% < 0.59 mm in X direction and E90% < 0.82 mm in Y direction. The tracking performance in X and Y direction was found to be equivalent. The physical decoupling of the leaf motion and the tracking motion is advantageous compared to DMLC tracking where substantial differences may arise between tracking of fast moving tumors inline and perpendicular to the MLC leaf trajectories (Sawant, 2008).

The 20 mm amplitude, 30 bpm sinus signal reaches a maximum speed of 20π mm/s which is even slightly exceeding the currently set maximum gimbals tracking speed of 60 mm/s. Patient signals usually consist of a first harmonic of below 0.25 Hz, but also contain higher harmonics and noise. As an illustration patient signal with a clinically relevant amplitude and frequency was applied to the Quasar phantom and tracked by the gimbals. For this particular patient the maximum speed was approximately 40 mm/s. With compensation of the system lag the tracking error was reduced to an E90% of 0.37 mm and RMSE of 0.20 mm. The maximum tracking error was reduced from 1.70 mm to 0.60 mm. Compared to previous reports on tracking errors with DMLC and robotic arm gantry real-time tracking, these preliminary values are promising, however, more verification is required on an extended patient dataset. In addition, the relationship between tracking error and dosimetric coverage of the tumor needs to be thoroughly investigated to establish certain minimum constraints on tracking error for clinical application.

REFERENCES

Wulf J., Baier K., Meuller G., et al. (2005). Dose-response in stereotactic irradiation of lung tumors. *Radioth. Oncol.* 77, 83-87

McGarry R., Papiez L., Williams M., et al. (2005)Stereotectic body radiation therapy of early-stage non-small-cell lung carcinoma: Phase I study. *Int J Radiat Oncol Biol Phys* 63, 1010-1015

Komaki R., Swann R., Ettinger D., et al. (2005). Phase I study of thoracic radiation dose escalation with concurrent chemotherapy for patients with limited small-cell lung cancer: Report of Radiation Therapy Oncology Group (RTOG) protocol 97-12. *Int J Radiat Oncol Biol Phys* 62, 342-350

Kwa S., Lebesque J., Theuws J., et al. (1998). Radiation pneumonitis as a function of mean lung dose: an analysis of pooled data of 540 patients. *Int J Radiat Oncol Biol Phys* 42, 1-9

M. Hernando, L. Marks, G. Bentel, et al. (2001). Radiation-induced pulmonary toxicity: a dose-volume histogram analysis in 201 patients with lung cancer. *Int J Radiat Oncol Biol Phys* 51, 650-659

D. Verellen, K. Tournel, J. Van de Steene, et al. (2006). Breathing-synchronized irradiation using stereoscopic kV-Imaging to limit influence of interplay between leaf motion and organ motion in 3D-CRT and IMRT: Dosimetric verification and first clinical experience. *Int J Radiat Oncol Biol Phys* 66, S108-S119

Wong J., Sharpe M., Jaffray D., et al. (1999). The use of active breathing control (ABC) to reduce margin for breathing motion. *Int J Radiat Oncol Biol Phys,* 44, 911-919

Mah D., Hanley J., Rosenzweig K., et al. (2000) Technical aspects of the deep inspiration breath-hold technique in the treatment of thoracic cancer. *Int J Radiat Oncol Biol Phys* 48, 1175-1185

D'Souza W. and McAvoy T. (2006). An analysis of the treatment couch and control system dynamics for respiration-induced motion compensation. *Med. Phys.* (33), 4701-4709

Putra, D.; Skworcow, P.; Haas, O.C.L.; Burnham, K.J.; Mills, J.A. (2007). Output-feedback tracking for tumour motion compensation in adaptive radiotherapy, *American Control Conference*, p 3414-19

Keall P., Cattell H., Pokhrel D., et al. (2006). Geometric accuracy of a real-time target tracking system with dynamic multileaf collimator tracking system. *Int J Radiat Oncol Biol Phys*, 65, 1579-1584

Tacke M., Nill S., Krauss A.. et al. (2010). Real-time tumor tracking: Automatic compensation of target motion using the Siemens 160 MLC. *Med. Phys.* 37, 753-761

Sawant A., Venkat R., Srivastava V., et al. (2008). Management of three-dimensional intrafraction motion through real-time DMLC tracking. *Med. Phys.* 35, 2050-2061

Hoogeman M., Prévost J., Nuyttens J., et al. (2009). Clinical accuracy of the respiration tumor tracking system of the CyberKnife: Assessment by analysis of log files. *Int J Radiat Oncol Biol Phys* 74, 297-303

Kamino Y., Takayama K., Kokubo M., et al. (2006). Development of a four-dimensional image-guided radiotherapy system with a gimbaled X-ray head. *Int J Radiat Oncol Biol Phys* 66, 271-278.

Keall P., Mageras G., Balter J., et al. (2006). The management of respiratory motion in radiation oncology report of AAPM 76. *Med. Phys.* 33, 3874-3900.

Wilbert J., Meyer J., Baier K., Guckenberger M., Herrmann C., Hess R., Janka C., Lei Ma, Mersebach T., Richter A., Roth M., Schilling K., Flentje M. (2008). Tumor tracking and motion compensation with an adaptive tumor tracking system (ATTS): system description and prototype testing, *Medical Physics*, 35(9), 3911-21.

Skworcow P., Putra D., Sahih A., Goodband J., Haas O.C.L., Burnham K.J., Mills J.A. (2007). Predictive tracking for respiratory induced motion compensation in adaptive radiotherapy, *Measurement and Control*, 40(1), 16-19.

Duda, R. O. and Hart P. E. (1972) Use of the Hough Transformation to Detect Lines and Curves in Pictures, *Comm. ACM, 15*, 11–15.